Volume 1 | Number 1 | Jan 2013 | Pages 1–100

Dalton Transactions

An international journal of inorganic chemistry
www.rsc.org/dalton

ROYAL SOCIETY OF CHEMISTRY

ROYAL SOCIETY OF CHEMISTRY

www.rsc.org/dalton

Journal Name

ARTICLE

Tetrahedral M[II] based binuclear double-stranded helicates: single-ion-magnet and fluorescent behaviour

Amit Kumar Mondal,[⊥] Vijay Singh Parmar,[⊥¥] Soumava Biswas, Sanjit Konar*

A rare class of dinuclear double-stranded helicates having tetrahedral metal centres with formulae of $[Co_2(L^1)_2] \cdot 2$ (CH_3CN) (**1**), $[Co_2(L^2)_2] \cdot 6$ (CH_3CN) (**2**), $[Zn_2(L^1)_2] \cdot 2$ $(CH_3CN) \cdot (CH_3OH)$ (**3**) and $[Zn_2(L^2)_2] \cdot 4$ (CH_3CN) (**4**) were synthesized and characterized. Detailed dc and ac magnetic susceptibility measurements reveal the presence of field induced slow magnetic relaxation behaviour in the high spin tetrahedral Co^{II} centres with an easy-plane magnetic anisotropy. Complexes **1** and **2** are the rare examples of transition metal based helicates showing such behaviour. Furthermore, **3** and **4** exhibit fluorescence emission in different solvent that are analyzed in terms of fluorescence quantum yields and lifetimes.

Introduction

Helices are the central structural motif in biological molecules such as the α-helical protein (single helix), DNA (double helix), and collagens (triple helix). A substantial effort has been made in the design and synthesis of artificial helical molecules, through metal coordination, hydrogen bonding, π-stacking, in order to mimic these biomacromolecules both structurally and functionally.[1] Over the past few decades, helicates have attracted tremendous research interest not only because of their aesthetically pleasing structural beauty[1e,f] but also for their potential applications in chiral catalysis, enantioselective processes, supramolecular devices and magnetic materials.[2-5] The chemical structures of helicates can be modulated by use of a variety of ligands containing two or more metal chelating sites that are connected to each other by a spacer.[6-9] The standard synthetic methods of helicates involve the use of metal-ion induced self-assembly of ligands which contains the repeating donor units of certain denticity, so that the binding abilities of the ligands need to match the coordination requirements of the metal ions. Most of the self-assembled multistranded helicates are binuclear, with some examples of trinuclear analogues,[10c] while those with more metal centers remain very rare.[10] Although a large number of double- and triple-stranded helicates have been reported using ditopic or tritopic ligands,[6] designing molecular assemblies with interesting diverse magnetic,[5] as well as photophysical

properties[11] and the existence of both the properties in a single system, is still a challenging task. Therefore, the choice of suitable metal ions and ligand system is important to induce different intriguing properties in a single molecular system. From the magnetic point of view, when the distance between the metal centres within a helical structure is small, they can significantly interact with each other. If the metal centres are well separated, it leads to quenching of magnetic interactions between them, consequently each individual metal ion shows slow relaxation of the magnetization; that is, single ions can behave like magnets which are known as Single Ion Magnets (SIMs).[12] The most fascinating features of SIMs lie in the possible prediction of their magnetic anisotropy based on the basic principles of the ligand field theory. Most of the reported transition metal based SIMs,[13] one common feature is the low coordination number of the metal centres, where the single ion anisotropy is enriched due to the unrestricted orbital angular momentum by limiting the coordination number of the metal ion.[14] The majority of helicates show SIM behaviour are mainly based on lanthanide ions, whereas the transition metal based SIMs are relatively rare. Among 3d-SIMs, Co^{II} based complexes are mostly interesting because of their non-integer spin ground state,[15] which declines the probability of quantum tunnelling of magnetization (QTM).[16] Recently a few tetrahedral Co^{II} complexes have been reported to show slow magnetic relaxation behavior, as a consequence of either an easy axis or an easy plane anisotropy.[17] A rational approach to

tune the magnetization relaxation behavior of tetrahedral Co^{II} centres within a helical structure is yet to be achieved. With this in mind, herein we report two Co^{II} based binuclear helicates constructed using two different Schiff-base ligands H_4L^1 and H_4L^2. In this paper, the dynamic magnetization study of tetra-coordinate Co^{II} based double-stranded helicates namely; $[Co_2(L^1)_2] \cdot 2$ (CH_3CN) (**1**) and $[Co_2(L^2)_2] \cdot 6$ (CH_3CN) (**2**) has been reported and variations in slow relaxation of the magnetization behavior was explored. Furthermore, the luminescence properties of the zinc derivatives $[Zn_2(L^1)_2] \cdot 2$ ($CH_3CN) \cdot (CH_3OH)$ (**3**) and $[Zn_2(L^2)_2] \cdot 4$ (CH_3CN) (**4**) has been investigated.

Results and Discussion

Four dinuclear double-stranded helicates were constructed using two different Schiff-base ligands H_4L^1 and H_4L^2.

Structural Description of 1 and 2

Single-crystal X-ray analysis of **1** and **2** revealed that complexes **1** and **2** crystallize in the triclinic *P*-1 and monoclinic $P2_1/n$ space groups respectively (Table S1). Both the complexes consist of dinuclear distorted double-stranded helicates, in which two ligands wrap around the two metal centers (Fig. 1). In both the cases, ligand contains two identical bidentate chelating units (NO) (homotopic = same denticity, same connectivity, same donor atoms) dispersed along the helical strand in a meridional manner to saturate the stereochemical requirements around the Co^{II} centres. The main difference between the structures of **1** and **2** comes from the degree of distortion in the coordination polyhedron, from the ideal tetrahedral geometry. In complex **1**, the Co-O distances are in the range of 1.895(1)-1.901(1) Å, while the Co-N distances are slightly longer than former (1.987(2)-1.995(2) Å) (Table S2). However in complex **2**, the Co-O/Co-N distances are found in the range of 1.901(1)-1.922(1) Å/1.985(1)-2.003(1) Å, respectively. The N-Co-N/O-Co-O/N-Co-O bond angles are are listed in Table S3 which falls in the range of reported dinuclear Co^{II} helicates.[18] In both the cases, the Co^{II} centres adopt a distorted tetrahedral coordination geometry where pairs of phenoxo oxygen and imino nitrogen atoms are cis to each other. The distortion from the regular tetrahedral geometry can be described by an angular index (τ_4), defined by Houser *et al* as follows: $\tau_4 = [360 - (a + b)]/141$ (*a* and *b* are the two largest angles around a four-coordinate metal center).[19] In complex **1**, the calculated $\tau_4 = 0.97$ and 1.0, whereas in **2** the $\tau_4 = 1.05$ and 0.99, therefore the coordination geometry around the Co(1) and Co(2) centers in both complexes can be best described as trigonal pyramidal (Fig. S1). The helical twists of the ligands, as defined by the torsion angles Co(1)-N(1)-N(6)-Co(2) and Co(1)-N(2)-N(5)-Co(2), are 144.2° and 148.1° for **1**, however for complex **2**, the values are observed to be 141.2° and 150.3°. In both the cases, helicand adopts "pseudo-C" conformations and forms a double-stranded dinuclear
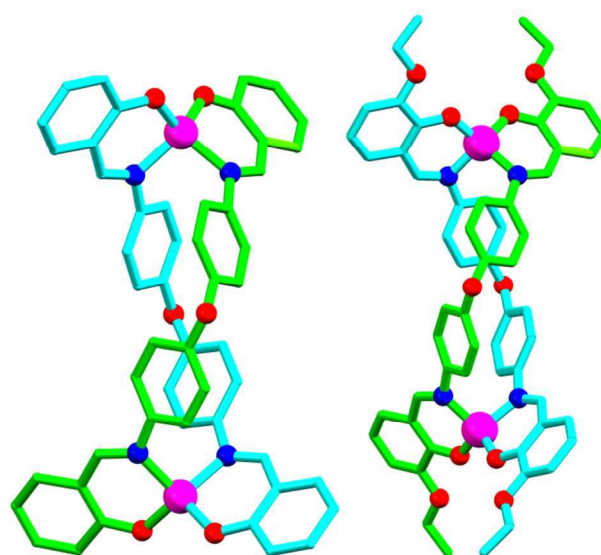
Fig. 1 View of the molecular structures of complex **1** (left) and complex **2** (right) illustrating double-stranded helicate formation. The two strands are differently coloured and hydrogen atoms are omitted for clarity.

helicate structure with a small cage in between them but the cage is empty because of the steric congestion. The intramolecular Co···Co distances are 11.68 Å and 11.67 Å for **1** and **2**, respectively (Fig. S2) and the C_2 axis passes through the Co···Co vector (Fig. S3). The phenyl rings from the diphenyl ether moieties of the two ligands are not parallel with each other and the values of the dihedral angles between them are 14.97° and 13.11° in **1**. Intramolecular $\pi\cdots\pi$ interactions are also noticed between the each pair phenyl rings with centroid to centroid distances of 4.051 Å and 4.125 Å (Fig. S4). The corresponding distances in **2** are longer (4.189 Å and 4.197 Å) (Fig. S4), and the dihedral angles are 19.53° and 17.29°. Furthermore, each of the independent $[Co_2(L^1)_2]$ complexes are inherently chiral and exhibits *P* for right-hand and *M* for left-hand helicity. Both the complexes crystallized in achiral space groups and the unit cell accommodates an equal amount of *P* and *M* enantiomers of the $[Co_2(L^1)_2]$ complexes, and hence resulting in a racemic solid containing equal amount of *P* and *M* configurations (Fig. S5-S6).

In both the complexes, there are significant π-interaction and intermolecular hydrogen-bonding network between the helicates and the interstitial solvent molecules, which supports the formation of a supramolecular arrangement. In complex **1**, hydrogen atoms of phenyl rings are involved in intermolecular hydrogen bonding (Table S4) with phenoxo oxygen atoms and lattice acetonitrile molecules and resulted in the formation of a supramolecular two dimensional arrangement (Fig. S7-S8). In complex **2**, lattice solvent molecules are involved in intermolecular hydrogen bonding (Table S5) with the phenyl rings and these interactions support the formation of a supramolecular two dimensional arrangement (Fig. S9-S10). In addition to the H-bonding interactions, strong CH···π interactions are also noticed with CH to centroid distances of 2.503 Å and 3.053 Å for **1** and **2**, respectively.

Structural Description of 3 and 4

The molecular structures of Zn-complexes **3** and **4** are very similar to that of the Co-complexes. Single-crystal X-ray analysis of **3** and **4** showed that complexes **3** and **4** crystallize in the triclinic *P*-1 and monoclinic *C*2/c space groups respectively (Table S1). Structures of the complexes reveal a neutral dinuclear helicate with a head-to-tail combination of the asymmetric dianionic iminophenols of the ligands.
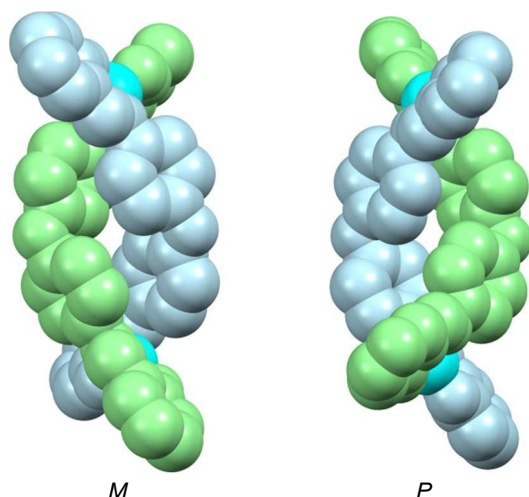
Fig. 2 Space-filling representations of the two independent [Zn₂(L¹)₂] complexes found in complex **3** with *M*- and *P*-helicity. The two strands are differently coloured and hydrogen atoms are omitted for clarity.

Intramolecular $\pi\cdots\pi$ interactions are also noticed between the each pair phenyl rings with centroid-to-centroid distances of 4.059 and 4.118 Å, with the dihedral angles of 14.81° and 21.95° for **3** (Fig. S11). The corresponding distances in **4** are slightly longer (4.127 Å), and the dihedral angles are 19.63° and 19.63° (Fig. S11). The intramolecular Zn···Zn distances are found to be 11.57 Å and 11.49 Å for **3** and **4**, respectively (Fig. S12). Both the complexes formed a racemic solid containing equal amount of *P* and *M* configurations (Fig. 2 and S13). Both the complexes are involved in intermolecular hydrogen bonding (Table S6-S7) with the lattice solvent molecules and these interactions support the formation of supramolecular two dimensional arrangement (Fig. S14-S17).

Magnetic Property Studies

Recently, it has been reported that the slow relaxation of the magnetization can be possible for mononuclear Co^{II} complexes, but the number of such systems is still limited in the literature.[17,20] To investigate the single-ion-magnetic behaviour of tetrahedral Co^{II} centers in **1** and **2**, detailed dc and ac susceptibility measurements has been performed. The purity of the as-synthesized products was shown by the good agreements of the bulk phase powder X-ray diffraction patterns with the

simulated one based on the single crystal structure data (Fig. S18-19). Magnetic susceptibility measurements were performed under direct current (DC) and an applied field of 0.1 T. At room temperature, the $\chi_M T$ values (χ_M = molar magnetic susceptibility) of 2.21 and 2.3 cm³ K mol⁻¹ were obtained for **1** and **2** respectively, which are larger than the spin-only value (1.875 cm³ mol⁻¹ K, S = 3/2, g = 2) for a high-spin Co^{II} ion.
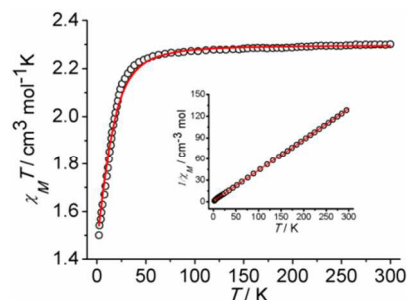
Fig. 3 $\chi_M T$ *vs.* *T* plot measured at 0.1 T for complex **2** and 1/χ_M *vs.* *T* plot shown in the inset. The red lines are the best fit.

These values fall well in the range of 2.1-3.4 cm³ mol⁻¹ K for the highly anisotropic Co^{II} ions with a significant orbital contribution.[21] Upon cooling from 300 K, the $\chi_M T$ values of **1** and **2** remains constant down to 75 K, below which it collapses, reaching a value of 1.42 and 1.5 cm³ mol⁻¹ K respectively at 2 K (Fig. 3 and S20). The decrease of the $\chi_M T$ curves at low temperature is may be due to the intrinsic magnetic anisotropy of the Co^{II} ions. Reduced magnetization data ($M/N\mu_B$ *vs.* *H*) were collected and it reached the highest values of 2.12 and 2.3 $N\mu_B$ for **1** and **2** respectively at 2 K and 7 T (Fig. 4). These values are well below the theoretical saturation for an *S* = 3/2 system (*M$_{sat}$* = 3.3 for g = 2.2). The magnetization values do
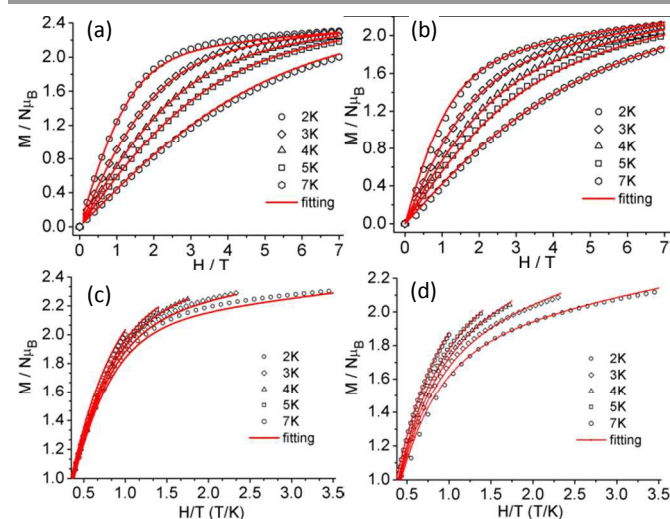
Fig. 4 $M/N\mu_B$ *vs.* *H* plots for complexes **1** (a) and **2** (b) at the indicated temperatures; Plots of $M/N\mu_B$ *vs.* *H/T* for complexes **1** (c) and **2** (d) at the indicated temperatures. The red lines are the best fit.

Journal Name

ARTICLE
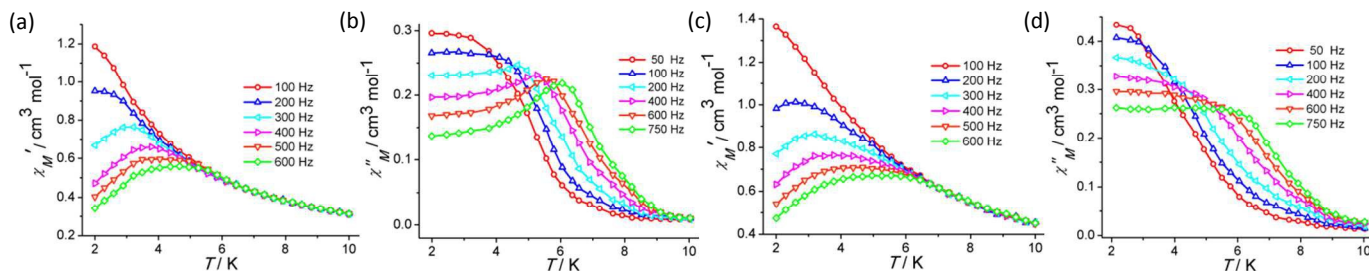
Fig. 5 (a) In-phase (χ_M') and (b) Out-of-phase (χ_M'') AC magnetic susceptibility plots for complex **1**; (c) In-phase (χ_M') and (d) Out-of-phase (χ_M'') AC magnetic susceptibility plots for complex **2** at 1000 Oe.

not saturate even at the highest available fields and the $M/N\mu_B$ *vs*. H/T plots show that all isotherm magnetization plots do not collapse on the same master curve indicating the highly magnetic anisotropic systems (Fig. 4). A spin Hamiltonian of eqn (1) is used to define the magnetic anisotropy qualitatively

$$H = g\mu_B S \times B + D[S_z^2 - S(S + 1)/3] + E(S_x^2 - S_y^2) \quad (1)$$

where μ_B, S and B represent the Bohr magneton, spin ($S = 3/2$ for **1** and **2**), and magnetic field vectors, respectively; D and E terms represent the single-ion axial and rhombic ZFS parameters. The PHI code[22] was employed to quantify the anisotropy parameters of the Co[II] centres by simultaneous fitting of the $\chi_M T$ *vs*. T and $M/N\mu_B$ *vs*. H plots and during the fitting procedure the g tensor was assumed to be isotropic. The best fits of the reduced magnetization data gave $D = 19.5$ cm^{-1}, $E = 0$, and g = 2.31 for **1**; $D = 16.2$ cm^{-1}, $E = 1.9 \times 10^{-3}$ cm^{-1}, and g = 2.22 for **2**. The results obtained for g and positive D values are consistent with those reported for other tetrahedral Co[II] complexes.[23] The positive sign of the ZFS parameter stems from the interaction between the ground and excited electronic states coupled through spin-orbit coupling.

To probe the magnetic relaxation dynamics of both the complexes, AC magnetic susceptibility measurements were performed in the temperature range of 1.8-10 K at a 3.5 Oe ac

field. No out-of-phase ac susceptibility (χ_M'') signal was observed for them under a zero dc field (Fig. S21-22). Nevertheless, upon application of a 1000 Oe dc field, all complexes show temperature- and frequency-dependent ac signals typically observed for field-induced 3d-SIM species (Fig. 5 and S23). Furthermore, the Cole-Cole plots (Fig. S24) were generated from the frequency-dependent ac susceptibility data. The fit of the χ_M'' *vs* χ_M' data at each temperature using the generalized Debye model[24a,b] yielded the values of α (this parameter determines the width of the distribution of relaxation times, so that $\alpha = 1$ corresponds to an infinitely wide distribution of relaxation times, whereas $\alpha = 0$ represents a relaxation with a single time constant) within the ranges 0.02-0.21 and 0.07-0.28 for **1** and **2**, respectively, suggesting the narrow distribution of the relaxation time. The effective energy barrier (U_{eff}) and relaxation times (τ_0) were determined using the Arrhenius eqn (2):[24c-i]

$$\ln(1/\tau) = \ln(1/\tau_0) - U_{eff}/kT \quad (2)$$

where k is the Boltzmann constant and $1/\tau_0$ is the pre-exponential factor. A linear fit to the high temperature data according to Arrhenius law afforded $U_{eff} = 20.5$ K and $\tau_0 = 1.2 \times 10^{-5}$ s for **1**; $U_{eff} = 11.2$ K and $\tau_0 = 1.7 \times 10^{-5}$ s for **2** (Fig. 6).
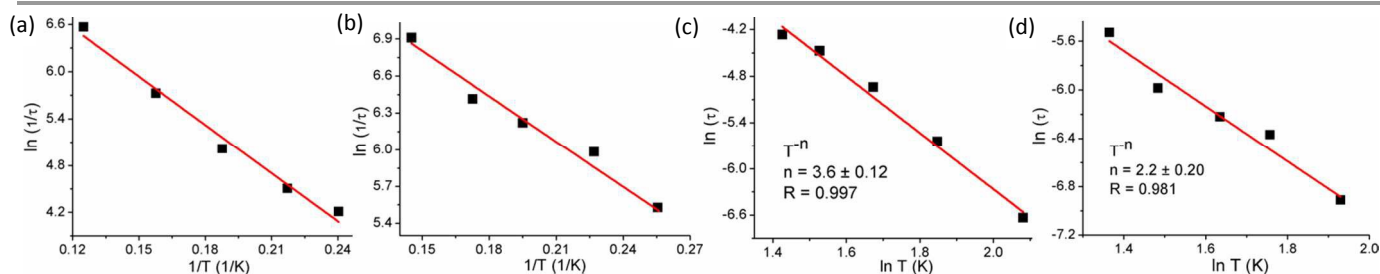
Fig. 6 ln (1/τ) *vs*. 1/T plots for complex **1** (a) and **2** (b). The red lines are the best fit of the Arrhenius relationship; Power law for complex **1** (c) and **2** (d) in the form ln(τ) *vs*. ln T.
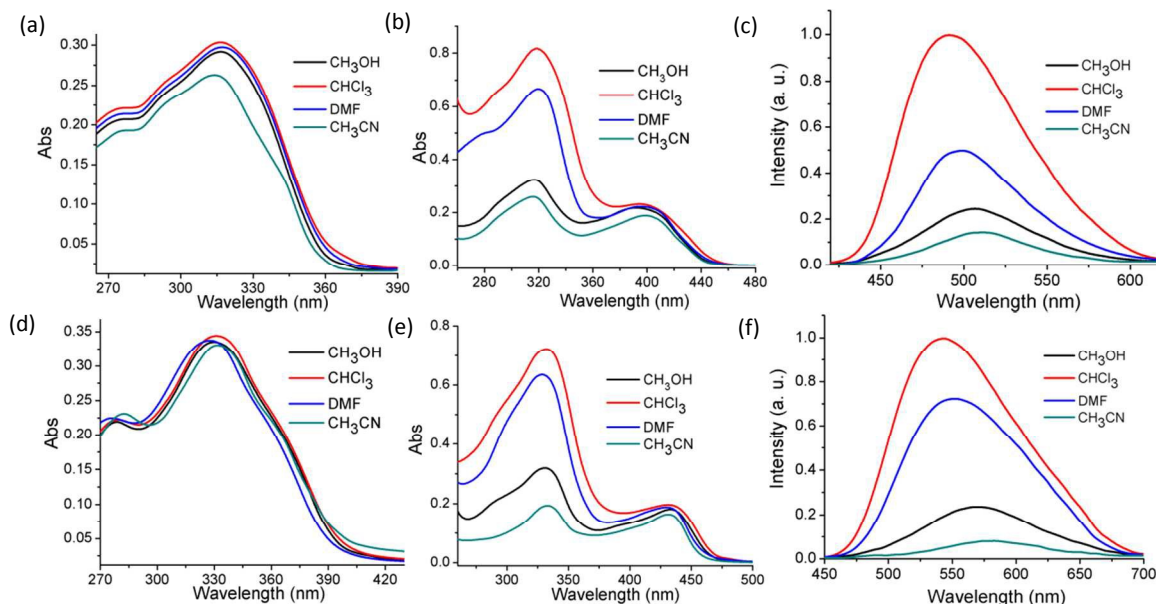
Fig. 7 Absorption spectra of the ligands H_4L^1 (a) and H_4L^2 (d); Absorption spectra of the zinc helicates **3** (b) and **4** (e) in different solvents; Fluorescence spectra of the zinc helicates **3** (c) and **4** (f).

The τ_0 values obtained for **1** and **2** are at the higher end of the experimental range found for SMMs[25] and are similar to those found for other Co[II] SIMs.[13] Recently, there have been two types of mechanisms responsible for the slow magnetic relaxation from a 3d metal system with a positive D value. The first one was suggested by Pardo *et al.*[13] They proposed that this type of slow relaxation arises from a transverse anisotropy barrier located in the easy (xy) plane, and the energy barrier is governed by a considerable E value. For our complexes, this mechanism does not applicable as the E values obtained experimentally are very close to zero. The other mechanism was based on a field-induced phonon bottleneck effect of the direct relaxation of the ground $M_S = \pm 1/2$ levels proposed by Luis *et al.*[26] As a matter of fact, the direct phonon-induced processes are strongly suppressed in a Kramers system with a significant anisotropy irrespective of the sign of D. Thus, magnetic relaxation has to occur either by the Orbach relaxation pathway through the excited $M_S = \pm 3/2$ levels[13] or by the optical or acoustic Raman process involving a virtual state.[26]

For both the complexes, as the obtained energy barriers are much lower than the energy gap between the $M_S = \pm 1/2$ and $M_S = \pm 3/2$ doublets, the Orbach pathway is not very likely. This fact is most likely due to the presence of a significant quantum pathway of relaxation at very low temperature which is not fully suppressed by the effects of the applied dc field. Additionally, the spin-lattice relaxation time can be expressed as:[27]

$$\tau^{-1} = AT + BT^n + C\exp(-\Delta/k_BT) \qquad (3)$$

The three terms respectively correspond to the direct, the Raman, and the Orbach process. In general, for Kramers ions n = 9, but when optical and acoustic phonons are considered, n = 1-6 is reasonable.[28] The relaxation times can be fitted to T^{-n} (Fig. 6), giving n = 3.6 and 2.2 for **1** and **2** respectively, which are close to the value reported for the Co-Y SIM by Colacio *et al.*[29] It suggests that the optical or acoustic Raman process have considerable contribution to the spin relaxation behaviour.

In order to investigate the effect of inter- and intramolecular exchange on the magnetic behavior, we have measured the effect of magnetic dilution on relaxation of the magnetization. To gain further insight into the relaxation process we prepared the diluted sample by using a mixture of $Zn(ClO_4)_2\cdot6H_2O$ and $Co(ClO_4)_2\cdot6H_2O$ in a 95:5 percentage ratio. The resulting complex contains three possible products namely, the Zn_2, ZnCo and Co_2 species. The probabilities of observing the different dinuclear species at the 5% cobalt dilution level are Zn_2: 90.25%, ZnCo: 9.5% and Co_2: 0.25%; therefore, the major paramagnetic product will be the single ion ZnCo species. For further characterization of diluted sample, energy dispersive X-ray spectroscopy (EDS) has been performed. EDS characterization of the diluted sample indicated the presence of Zn, Co, O and N elements in the sample (Fig. S25). AC susceptibility measurements were then carried out on a polycrystalline sample of the diluted complex. No significant difference was observed between the energy barrier of relaxation of the magnetization of the diluted sample compared to the undiluted one (Fig. S26). So, we may conclude that intermolecular forces and dipolar interactions are negligible; hence, the relaxations in the case of **1** and **2** are of single ion origin.

On comparative point of view, both the complexes (**1** and **2**) contain similar CoN_2O_2 cores; however their relaxation dynamic behaviors are slightly different. It is well-known that small structural changes around the metal centres played an important role in the difference in relaxation dynamics of the complexes.[30] The main difference between the structures of **1** and **2** comes from the degree of distortion in the coordination polyhedron, from the ideal tetrahedral geometry. Systematic analysis of the coordination geometries around the Co^{II} centres using SHAPE 2.1[31] reveals that the distortion from ideal geometry being greater in Co^{II} centres of complex **2** (minimum

CShM values of ~3.34 compared to ~2.15 for **1**, Table S8). Additionally, the Co-O and Co-N bond distances in **1** are shorter than those in complex **2** (Table S2) leads to stronger bonds in the former which resulted in a larger energy difference between the ground state and first excited state.[32a] Since it is difficult to describe the crystal field of Co^{II}, it can be only commented that the slightly different slow magnetization relaxation behaviors observed in **1** and **2** are possibly the result of small structural changes which are likely to affect the nature or directions of the easy axes.[32b,c]
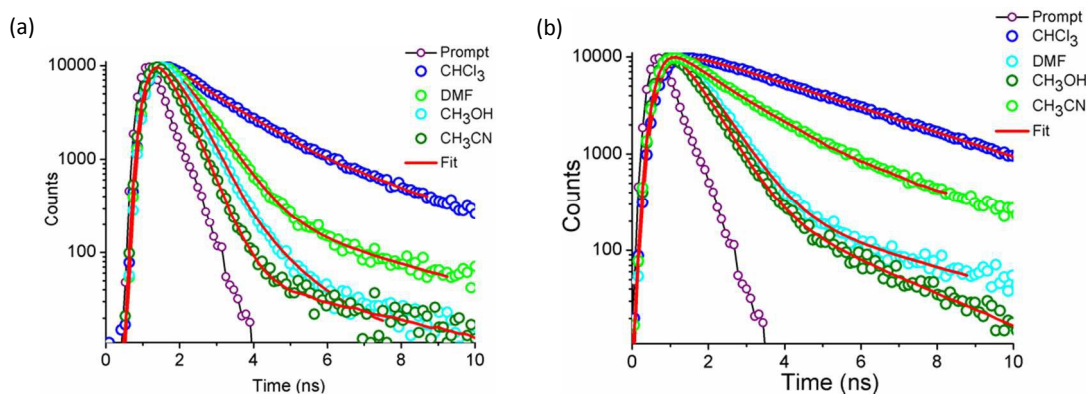
Fig. 8 Typical luminescence decay profiles observed for **3** (a) and **4** (b) and the red lines are the corresponding bi-exponential fits of **3** and **4**, respectively.

Table 1. Photophysical Parameters of the Zinc Helicates **3** and **4**.

Complex	Solvent	Φ	τ_1	A_1	τ_2	A_2	τ_{av}	χ^2
3	CHCl$_3$	0.097	0.824	2.68	3.318	97.32	3.25	1.09
	DMF	0.041	0.672	92.57	2.751	7.43	0.82	1.12
	MeOH	0.019	0.415	87.52	2.210	12.48	0.63	1.26
	MeCN	0.008	0.398	95.68	1.843	4.32	0.46	1.25
4	CHCl$_3$	0.113	1.242	5.50	3.980	94.50	3.82	1.01
	DMF	0.071	0.936	90.76	3.447	9.24	1.16	1.19
	MeOH	0.027	0.520	90.53	2.510	9.47	0.70	1.15
	MeCN	0.011	0.408	85.46	2.013	14.54	0.64	1.26

Photophysical Properties

The absorption band of the ligand H_4L^1 is located at 316 nm, due to the π-π^* transition from the iminophenol backbone,[33] and that is shifted to 330 nm for H_4L^2 ligand (Fig. 7). The solvent effect on the absorption spectra is negligible and both the ligands show no emission spectra upon excitation in the range of 315-330 nm. The absorption bands of complex **3** and **4** exhibits an additional band at around 400 and 430 nm respectively (Fig. 7), which can be attributed to the coordination with Zn^{II}.[33] The excitation spectra matches similarly with the absorption spectra for both the complexes and that confirms no geometry change occurs upon excitation.[34] On excitation at the wavelength of absorption maxima, the emission spectra of complex **3** and **4** consists of fluorescence band centered around 490 and 543 nm respectively (Fig. 7), which can be attributed to the π-π^* transitions of the metal perturbed ligand.[35] The presence of high intensity fluorescence spectra upon metal complexation can be described by the

increased conformational rigidity of the ligand within the complex, and that causes to a smaller degree of nonradiative deactivation.[36] Furthermore, the emission spectra of both the complexes strongly depend on the nature of the solvent, which indicates specific solvation of the complex in the excited state. To know about this dependence quantitatively, the solution-state quantum yields were determined using the following equation (4) [37]

$$\Phi_x = (I_x/I_{st})(A_{st}/A_x)(\eta_x^2/\eta_{st}^2)\Phi_{st} \qquad (4)$$

where, Φ_{st} is the quantum yield of the reference; I_x and I_{st} are the integrated areas under the emission spectra of the complex and the reference. A_x and A_{st} are the absorption coefficients of the complex and the reference (Quinine sulfate).[38] η_x and η_{st} are the refractive index of the solvent of the complex and reference, respectively. The obtained fluorescence quantum yields in chloroform (determined relative to that of Quinine sulfate) are 0.097 and 0.113 for complexes **3** and **4** respectively (Table 1).

The corresponding Φ values in other solvents (CH_3OH, CH_3CN and DMF) are being listed in Table 1.

The luminescence lifetime, τ, of two complexes in different solvents were calculated at room temperature using an excitation wavelength of 340 nm. The fluorescence decay curves of **3** and **4** (Fig. 8) can be well-fitted into a bi-exponential function such as [37]

$$I(t) = A_1\exp(-t/\tau_1)+A_2\exp(-t/\tau_2) \qquad (5)$$

where, $I(t)$ is the luminescence intensity at time t, A_1 and A_2 are the intensities at time t_1 and t_2, respectively, and τ_1 and τ_2 are the decay times for the exponential components, respectively. The decays are characterized by two lifetimes: a long component which is predominant in chloroform and is responsible for the stronger emission in this solvent, and a shorter component which is predominant in the other solvents. The average lifetime (τ_{av}) can be calculated by using the following equation,

$$\tau_{av} = (A_1\tau_1+A_2\tau_2)/(A_1+A_2) \qquad (6)$$

The average lifetime (τ_{av}) obtained in chloroform are 3.25 and 3.82 ns for complexes **3** and **4**, respectively. The corresponding τ and τ_{av} values in other solvents (CH_3OH, CH_3CN and DMF) are being listed in Table 1.

Conclusions

Our results demonstrate that slow magnetic relaxation can be achieved under an applied dc field in the high spin tetrahedral Co^{II} centres with an easy-plane magnetic anisotropy. To the best of our knowledge, this is the first example of a helicate based on transition metal ions showing such behaviour. The results also prove that the dynamic magnetic properties of transition metal based helicates can be tuned by structural modifications. Furthermore, the study of the Zn analogues reveal that they behave as potential candidates for photoluminescent materials.

Experimental Section

X-ray Crystallography

Intensity data were collected on a Brüker APEX-II CCD diffractometer using a graphite monochromated Mo-Kα radiation (α = 0.71073 Å) at 296 K. Data collections were performed using φ and ω scan. The structures were solved using direct methods followed by full matrix least square refinements against F^2 (all data HKLF 4 format) using SHELXTL.[39] A multi-scan absorption correction, based on equivalent reflections was applied to the data. Anisotropic refinement was used for all non-hydrogen atoms. Hydrogen atoms were placed in appropriate calculated positions. In complexes **2** and **4**, during the final stages of refinement, some Q peaks having high electron densities were found, which corresponding to disordered solvent molecules and hence are

squeezed out using the SQUEEZ program in PLATON. From the TG analysis (Fig. S27), we have calculated that in complex **2**, six CH_3CN molecules are present (calc. 18.1%; found 17.6%), whereas in **4** two CH_3CN molecules are present (calc. 6.8%; found 6.6%), and hence these are included in the molecular formula and accordingly the molecular weights have been corrected and mentioned in the crystallographic table (Table S1). Crystallographic data for complexes **1-4** were summarized in Table S1.

Materials and Methods

All chemicals were of reagent grade and used without further purification. The elemental analyses were carried out on Elementar Microvario Cube Elemental Analyzer. FT-IR spectra (4000−400 cm^{-1}) were recorded on KBr pellets with a Perkin-Elmer Spectrum BX spectrometer. Powder X-ray diffraction (PXRD) data were collected on a PANalytical EMPYREAN instrument using Cu-Kα radiation. Magnetic measurements were performed using a SQUID VSM magnetometer (Quantum Design). The measured values were corrected for the experimentally measured contribution of the sample holder, while the derived susceptibilities were corrected for the diamagnetism of the samples, estimated from Pascal's tables.[40] The photoluminescence spectral measurements were recorded on a HORIBA JOBIN YVON FLUOROMAX-4 spectrofluorometer. The fluorescence lifetime measurements were performed using a Hamamatsu MCP photomultiplier. The time-correlated single photon counting (TCSPC) setup consists of an Ortec 9327 pico-timing amplifier and using pulse Diode laser (NanoLED, N-340) for excitation (λ_{ex} = 340 nm) with a setup target 10,000 count. The instrument response function (IRF) was measured before and after fluorescence lifetime measurement using a dilute suspension of Ludox (purchased from Sigma) colloidal silica. The emission polarizer was positioned at magic angle (54.7º) polarization with respect to excitation polarizer. Single and multi-exponential fitting functions were employed by iterative deconvolution method using supplied DAS software. The diluted sample was directly sprinkled on conductive carbon tape and coated with gold by sputter coating for 2 min. They were visualized under a scanning electron microscope (SEM) at a working voltage of 20 kV. The EDS was performed at a working voltage of 20 kV and was standardized with the Co element.

Synthesis

Synthesis of ligand

Ligand H_4L^1 and H_4L^2 were synthesized following the previously reported procedures.[41]

$[Co_2(L^1)_2]\cdot2 (CH_3CN)$ (1)

41 mg (0.1 mmol) of ligand H_4L^1 and 37 mg (0.1 mmol) of $Co(ClO_4)_2\cdot6H_2O$ were taken acetonitrile/methanol mixture (2:1, 10 mL) and the reaction mixture was stirred for 30 mins. Then triethylamine (0.2 mmol, 20 mg) was added this reaction mixture which was rapidly stirred for 3 hrs. Red coloured single

crystals of **1** were obtained in 65% yield by slow evaporation of the reaction mixture over 3 days at room temperature in air. Elemental analysis: calcd. (%) for $C_{56}H_{42}Co_2N_6O_6$: C 66.41, N 8.30, H 4.18; found C 66.56, N 8.21, H 4.25. Selected IR data (KBr pellet; cm^{-1}): 1665(m), 1601(m), 1537(w), 1489(s), 1431(m), 1382(w), 1235(s), 1186(s), 857(w).

$[Co_2(L^2)_2]\cdot6$ (CH$_3$CN) (2)

50 mg (0.1 mmol) of ligand H$_4$L^2 and 37 mg (0.1 mmol) of Co(ClO$_4$)$_2$·6H$_2$O were taken acetonitrile/methanol mixture (2:1, 10 mL) and the reaction mixture was stirred for 30 mins. Then triethylamine (0.2 mmol, 20 mg) was added this reaction mixture which was rapidly stirred for 4 hrs. Red coloured single crystals of **2** were obtained in 53% yield by slow evaporation of the reaction mixture over 2 days at room temperature in air. Elemental analysis: calcd. (%) for $C_{72}H_{70}Co_2N_{10}O_{10}$: C 63.91, N 10.35, H 5.21; found C 64.02, N 10.41, H 5.30. Selected IR data (KBr pellet; cm^{-1}): 1662(m), 1608(m), 1542(w), 1495(m), 1461(m), 1435(m), 1385(w), 1237(s), 1182(s), 855(w).

$[Zn_2(L^1)_2]\cdot2$ (CH$_3$CN)·(CH$_3$OH) (3)

41 mg (0.1 mmol) of ligand H$_4$L^1 and 38 mg (0.1 mmol) of Zn(ClO$_4$)$_2$·6H$_2$O were taken acetonitrile/methanol mixture (2:1, 10 mL) and the reaction mixture was stirred for 30 mins. Then triethylamine (0.2 mmol, 20 mg) was added this reaction mixture which was rapidly stirred for 3 hrs. Yellow coloured single crystals of **3** were obtained in 71% yield by slow evaporation of the reaction mixture over one week at room temperature in air. Elemental analysis: calcd. (%) for $C_{57}H_{46}Zn_2N_6O_7$: C 64.72, N 7.94, H 4.38; found C 64.83, N 8.01, H 4.26. Selected IR data (KBr pellet; cm^{-1}): 1660(m), 1605(m), 1539(w), 1485(s), 1437(m), 1380(w), 1233(s), 1185(s), 851(w).

$[Zn_2(L^2)_2]\cdot4$ (CH$_3$CN) (4)

50 mg (0.1 mmol) of ligand H$_4$L^2 and 38 mg (0.1 mmol) of Zn(ClO$_4$)$_2$·6H$_2$O were taken acetonitrile/methanol mixture (2:1, 10 mL) and the reaction mixture was stirred for 30 mins. Then triethylamine (0.2 mmol, 20 mg) was added this reaction mixture which was rapidly stirred for 4 hrs. Yellow coloured single crystals of **4** were obtained in 61% yield by slow evaporation of the reaction mixture over one week at room temperature in air. Elemental analysis: calcd. (%) for $C_{68}H_{64}Zn_2N_8O_{10}$: C 63.61, N 8.72, H 5.02; found C 63.75, N 8.81, H 5.12. Selected IR data (KBr pellet; cm^{-1}): 1663(m), 1602(m), 1541(w), 1492(m), 1458(m), 1434(m), 1381(w), 1235(s), 1179(s), 857(w).

Preparation of Diluted Sample:

The diluted sample was prepared by a similar procedure to that for complex **1**, but using a mixture of Zn(ClO$_4$)$_2$·6H$_2$O and Co(ClO$_4$)$_2$·6H$_2$O in a 95:5 percentage ratio. The obtained doped level in the final product was tested by energy dispersive X-ray spectroscopy (EDS). EDS characterization of the diluted sample indicated the presence of Zn, Co, O and N elements in the sample (Fig. S25).

Corresponding Author

E-mail: skonar@iiserb.ac.in

Notes and references

Department of Chemistry, IISER Bhopal, Bhopal 462066, MP, India.
E-mail: skonar@iiserb.ac.in; Fax: +91-7556692392; Tel: +91-755 6692339.
$^\perp$*Equal contribution*
¥ *Undergraduate Researcher*

1. (*a*) E. Yashima, K. Maeda, H. Iida, Y. Furusho and K. Nagai, *Chem. Rev.*, 2009, **109**, 6102; (*b*) E. Yashima, K. Maeda and Y. Furusho, *Acc. Chem. Res.*, 2008, **41**, 1166; (*c*) H. Juwarker, J. M. Suk and K. S. Jeong, *Chem. Soc. Rev.*, 2009, **38**, 3316; (*d*) B.-B. Ni, Q. Yan, Y. Ma and D. Zhao, *Coord. Chem. Rev.*, 2010, **254**, 954; (*e*) J.-M. Lehn, A. Rigault, J. Siegel, J. Harrowfield, B. Chevrier and D. Moras, *Proc. Natl. Acad. Sci. USA*, 1987, **84**, 2565; (*f*) S. Li, C. Jia, B. Wu, Q. Luo, X. Huang, Z. Yang, Q.-S. Li and X.-J. Yang, *Angew. Chem. Int. Ed.*, 2011, **50**, 5721.

2. (*a*) H. Sleiman, P. Baxter, J.-M. Lehn and K. Rissanen, *J. Chem. Soc., Chem. Commun.*, 1995, 715; (*b*) J.-C. Chambron, C. O. Dietrich-Buchecker, J.-F. Nierengarten, J.-P. Sauvage, N. Solladié, A.-M. Albrecht-Gary and M. Meyer, *New J. Chem.*, 1995, **19**, 409; (*c*) G. S. Hanan, C. R. Arana, J.-M. Lehn and D. Fenske, *Angew. Chem., Int. Ed. Engl.*, 1995, **34**, 1122; (*d*) P. Baxter, G. S. Hanan and J.-M. Lehn, *Chem. Commun.*, 1996, 2019; (*e*) P. Baxter, J.-M. Lehn, J. Fischer and M. T. Youinou, *Angew. Chem., Int. Ed. Engl.*, 1994, **33**, 2284; (*f*) J.-P. Sauvage, *Acc. Chem. Res.*, 1990, **23**, 319; (*g*) C. O. Dietrich-Buchecker and J.-P. Sauvage, *Chem. Rev.*, 1987, **87**, 795.

3. (*a*) M. D. Pluth, R. G. Bergman and K. N. Raymond, *Selective Stoichiometric and Catalytic Reactivity in the Confines of a Chiral Supramolecular Assembly, Chapter in Supramolecular Catalysis*, ed. Piet W. N. M. van Leeuwen,Wiley-VCH, 2008, p. 165; (*b*) K.-C. Sham, H.-L. Yeung, S.-M. Yiu, T.-C. Lau and H.-L. Kwong, *Dalton Trans.*, 2010, **39**, 9469; (*c*) W. Xuan, M. Zhang, Y. Liu, Z. Chen and Y. Cui, *J. Am. Chem. Soc.*, 2012, **134**, 6904; (*d*) D. Fiedler, D. H. Leung, R. G. Bergman and K. N. Raymond, *Acc. Chem. Res.*, 2005, **38**, 351; (*e*) R. Kaminker, X. de Hatten, M. Lahav, F. Lupo, A. Gulino, G. Evmenenko, P. Dutta, C. Browne, J. R. Nitschke and M. E. van der Boom, *J. Am. Chem. Soc.*, 2013, **135**, 17052.

4. F. R. Keene, *Chirality. Supramolecular Chemistry: From Molecules to Nanomaterials,* 2012.

5. (*a*) M. Vázquez, A. Taglietti, D. Gatteschi, L. Sorace, C. Sangregorio, A. M. González, M. Maneiro, R. Pedrido and M. R. Bermejo, *Chem. Commun.*, 2003, 1840; (*b*) C. J. Matthews, S. T. Onions, G. Morata, L. J. Davis, S. L. Heath and D. J. Price, *Angew. Chem., Int. Ed.*, 2003, **42**, 3166; (*c*) D. Pelleteret, R. Clérac, C. Mathoniére, E. Harté, W. Schmitt and P. E. Kruger, *Chem. Commun.*, 2009, 221; (*d*) G. Novitchi, J.-P. Costes, J.-P. Tuchagues, L. Vendier and W. Wernsdorfer, *New J. Chem.*, 2008, **32**, 197; (*e*) A. Adhikary, H. S. Jena and S. Konar, *Dalton Trans.*, 2015, **44**, 15531.

6. (*a*) M. A. Mateos-Timoneda, M. Crego-Calama and D. N. Reinhoudt, *Chem. Soc. Rev.*, 2004, **33**, 363; (*b*) M. J. Hannon and L. J. Childs, *Supramol. Chem.*, 2004, **16**, 7.

7. (*a*) O. Mamula and A. von Zelewsky, *Coord. Chem. Rev.*, 2003, **242**, 87; (*b*) M. Albrecht, *Chem. Rev.*, 2001, **101**, 3457; (*c*) A. von Zelewsky and O. Mamula, *J. Chem. Soc. Dalton Trans.*, 2000, 219; (*d*) M. Albrecht, *Chem. – Eur. J.*, 2000, **6**, 3485; (*e*) A. von Zelewsky, *Coord. Chem. Rev.*, 1999, **190**, 811.

8. (*a*) U. Knof and A. von Zelewsky, *Angew. Chem.*, *Int. Ed.*, 1999, **38**, 302; (*b*) D. L. Caulder and N. Raymond, *Acc. Chem. Res.*, 1999, **32**, 975; (*c*) M. Albrecht, *Chem. Soc. Rev.*, 1998, **27**, 281; (*d*) C. Piguet, G. Bernardinelli and G. Hopfgartner, *Chem. Rev.*, 1997, **97**, 2005.

9. (*a*) J. D. Watson and F. H. C. Crick, *Nature*, 1953, **171**, 737; (*b*) W. Saenger, *Principles of Nucleic Acid Structure*, Springer, New York, 1984; (*c*) F. Cramer, *Chaos and Order*, *The Complex Structure of Living Systems*, VCH, Weinheim, 1993.

10. (*a*) C. Piguet, G. Bernardinelli and G. Hopfgartner, *Chem. Rev.*, 1997, **97**, 2005; (*b*) M. Albrecht, *Chem. Soc. Rev.*, 1998, **27**, 281; (*c*) M. Albrecht, *Chem. Rev.*, 2001, **101**, 3457; (*d*) M. J. Hannon and L. J. Childs, *Supramol. Chem.*, 2004, **16**, 7; (*e*) C. Piguet, M. Borkovec, J. Hamacek and K. Zeckert, *Coord. Chem. Rev.*, 2005, **249**, 705.

11. (*a*) S. Floquet, N. Ouali, B. Bocquet, G. Bernardinelli, D. Imbert, J. C. G. Bünzli, G. Hopfgartner and C. Piguet, *Chem.—Eur. J.*, 2003, **9**, 8; (*b*) M. Z. Albrecht, *Anorg. Allg. Chem.*, 2010, **636**, 2198; (*c*) M. Albrecht, O. Osetska, J. C. G. Bünzli, F. Gumy and R. Fröhlich, *Chem.—Eur. J.*, 2009, **15**, 8791; (*d*) C. D. B. Vandevyver, A.-S. Chauvin, S. Comby and J. C. G. Bünzli, *Chem. Commun.*, 2007, 1716; (*e*) V. Fernández-Moreira, B. Song, V. Sivagnanam, A.-S. Chauvin, C. D. B. Vandevyver, M. Gijs, I. Hemmilä, H.-A. Lehr and J. C. G. Bünzli, *Analyst*, 2010, **135**, 42; (*f*) A.-S. Chauvin, S. Comby, M. Baud, C. De Piano, C. Duhot and J. C. G. Bünzli, *Inorg. Chem.*, 2009, **48**, 10687; (*g*) M. Elhabiri, R. Scopelliti, J. C. G. Bünzli and C. J. Piguet, *J. Am. Chem. Soc.*, 1999, **121**, 10747; (*h*) F. Stomeo, C. Lincheneau, J. P. Leonard, J. E. O'Brien, R. D. Peacock, C. P. McCoy and T. Gunnlaugsson, *J. Am. Chem. Soc.*, 2009, **131**, 9636; (*i*) S. V. Eliseeva, G. Auböck, F. van Mourik, A. Cannizzo, B. Song, E. Deiters, A.-S. Chauvin, M. Chergui and J. C. G. Bünzli, *J. Phys. Chem. B*, 2010, **114**, 2932.

12. (*a*) F. Habib and M. Murugesu, *Chem. Soc. Rev.*, 2013, **42**, 3278; (*b*) D. N. Woodruff, R. E. P. Winpenny and R. A. Layfield, *Chem. Rev.*, 2013, **113**, 5110; (*c*) A. K. Mondal, S. Goswami and S. Konar, *Dalton Trans.*, 2015, **44**, 5086; (*d*) S. Goswami, A. K. Mondal and S. Konar, *Inorg. Chem. Front.*, 2015, **2**, 687.

13. (*a*) W. H. Harman, T. D. Harris, D. E. Freedman, H. Fong, A. Chang, J. D. Rinehart, A. Ozarowski, M. T. Sougrati, F. Grandjean, G. J. Long, J. R. Long and C. J. Chang, *J. Am. Chem. Soc.*, 2010, **132**, 18115; (*b*) D. Weismann, Y. Sun, Y. Lan, G. Wolmershäuser, A. K. Powell and H. Sitzmann, *Chem. - Eur. J.*, 2011, **17**, 4700; (*c*) P. H. Lin, N. C. Smythe, S. I. Gorelsky, S. Maguire, N. J. Henson, I. Korobkov, B. L. Scott, J. C. Gordon, R. T. Baker and M. Murugesu, *J. Am. Chem. Soc.*, 2011, **133**, 15806; (*d*) S. Mossin, B. L. Tran, D. Adhikari, M. Pink, F. M. Heinemann, J. Sutter, R. K. Szilagyi, K. Meyer and D. J. Mindiola, *J. Am Chem. Soc.*, 2012, **134**, 13651; (*e*) J. M. Zadrozny, M. Atanasov, A. M. Bryan, C. Y. Lin, B. D. Rekken, P. P. Power, F. Neese and J. R. Long, *Chem. Sci.*, 2013, **4**, 125; (*f*) T. Jurca, A. Farghal, P. H. Lin, I. Korobkov, M. Murugesu and D. S. Richardson, *J. Am. Chem. Soc.*, 2011, **133**, 15814; (*g*) J. M. Zadrozny and J. R. Long, *J. Am. Chem. Soc.*, 2011, **133**, 20732; (*h*) J. Vallejo, I. Castro, R. R. García, J. Cano, M. Julve, F. Lloret, G. D. Munno, W. Wernsdorfer and E. Pardo, *J. Am. Chem. Soc.*, 2012, **134**, 15704; (*i*) G. A. Craig and M. Murrie, *Chem. Soc. Rev.*, 2015, **44**, 2135; (*j*) R. Ruamps, R. Maurice, L. Batchelor, M. Boggio-Pasqua, R. Guillot, A. L. Barra, J. J. Liu, E. Bendeif, S. Pillet, S. Hill, T. Mallah and N. Guihery, *J. Am. Chem. Soc.*, 2013, **135**, 3017; (*k*) S. Gómez-Coca, E. Cremades, N. Aliaga-Alcalde and E. Ruiz, *Inorg. Chem.*, 2014, **53**, 676; (*l*) S. Vaidya, A. Upadhyay, S. K. Singh, T. Gupta, S. Tewary, S. K. Langley, J. P. S. Walsh, K. S. Murray, G. Rajaraman and M. Shanmugam, *Chem. Commun.*, 2015, **51**, 3739; (*m*) S. Gómez-Coca, D. Aravena, R. Morales and E. Ruiz, *Coord. Chem. Rev.*, 2015, **289**,

379; (*n*) A. K. Bar, C. Pichon and J. Sutter, *Coord. Chem. Rev.* 2015, doi:10.1016/j.ccr.2015.06.013.

14. (*a*) J. M. Zadrozny, D. J. Xiao, M. Atanasov, G. J. Long, F. Grandjean, F. Neese and J. R. Long, *Nat. Chem.*, 2013, **5**, 577; (*b*) R. C. Poulten, M. J. Page, A. G. Algarra, J. J. Le Roy, I. Lopez, E. Carter, A. Llobet, S. A. Macgregor, M. F. Mahon, D. M. Murphy, M. Murugesu and M. K. Whittlesey, *J. Am. Chem. Soc.*, 2013, **135**, 13640.

15. (*a*) A. Caneschi, D. Gatteschi, N. Lalioti, C. Sangregorio, R. Sessoli, G. Venturi, A. Vindigni, A. Rettori, M. G. Pini and M. A. Novak, *Angew. Chem., Int. Ed.*, 2001, **40**, 1760; (*b*) M. Murrie, *Chem. Soc. Rev.*, 2010, **39**, 1986; (*c*) M. G. Pini, A. Rettori, L. Bogani, A. Lascialfari, M. Mariani, A. Caneschi and R. Sessoli, *Phys. Rev. B: Condens. Matter Mater. Phys.*, 2011, **84**, 094444.

16. H. A. Kramers, *Proc. R. Acad. Sci. Amsterdam*, 1930, **33**, 959.

17. (*a*) J. M. Zadrozny and J. R. Long, *J. Am. Chem. Soc.*, 2011, **133**, 20732; (*b*) F. Yang, Q. Zhou, Y. Q. Zhang, G. Zeng, G. H. Li, Z. Shi, B. W. Wang and S. H. Feng, *Chem. Commun.*, 2013, **49**, 5289; (*c*) J. Valejo, I. Castro, R. Ruiz-Garcia, J. Cano, M. Julve, F. Lloret, G. de Munno, W. Wernsdorfer and E. Pardo, *J. Am. Chem. Soc.*, 2012, **134**, 15704.

18. (*a*) H.-W. Xu, J.-X. Li and Y.-H. Li, *ActaCrystallogr.*, 2008, **E64**, o1145; (*b*) P. Cucos, F. Tuna, L. Sorace, I. Matei, C. Maxim, S. Shova, R. Gheorghe, A. Caneschi, M. Hillebrand and M. Andruh, *Inorg. Chem.*, 2014, **53**, 7738; (*c*) B. Chakraborty, P. Halder, S. Chakraborty, O. Das and S. Paria, *InorganicaChimicaActa*, 2012, **387**, 332.

19. L. Yang, D. R. Powell and R. P. Houser, *Dalton Trans.*, 2007, 955.

20. Y.-Y. Zhu, C. Cui, Y.-Q. Zhang, J.-H. Jia, X. Guo, C. Gao, K. Qian, S.-D. Jiang, B.-W. Wang, Z.-M. Wang and S. Gao, *Chem. Sci.*, 2013, **4**, 1802.

21. F. E. Mabbs and D. J. Machin, *Magnetism and Transition Metal Complexes*; Dover Publications: Mineola, NY, 2008.

22. N. F. Chilton, R. P. Anderson, L. D. Turner, A. Soncini and K. S. Murray, *J. Comput. Chem.*, 2013, **34**, 1164.

23. (*a*) S. Vaidya, A. Upadhyay, S. K. Singh, T. Gupta, S. Tewary, S. K. Langley, J. P. S. Walsh, K. S. Murray, G. Rajaraman and M. Shanmugam, *Chem. Commun.*, 2015, **51**, 3739; (*b*) L. Smolko, J. Černák, M. Dušek, J. Miklovič, J. Titiš and R. Boča, *Dalton Trans.*, 2015, **44**, 17565; (*c*) J. M. Zadrozny, J. Liu, N. A. Piro, C. J. Chang, S. Hill and J. R. Long, *Chem. Commun.*, 2012, **48**, 3927; (*d*) W. Huang, T. Liu, D. Wu, J. Cheng, Z. W. Ouyang and C. Duan, *Dalton Trans.*, 2013, **42**, 15326.

24. (*a*) K. S. Cole and R. H. Cole, *J. Chem. Phys.*, 1941, **9**, 341; (*b*) Y.-N. Guo, G.-F. Xu, Y. Guo and J. Tang, *Dalton Trans.*, 2011, **40**, 9953; (*c*) S. Xue, Y. N. Guo, L. Zhao, P. Zhang and J. Tang, *Dalton Trans.*, 2014, **43**, 1564; (*d*) R. V. Chamberlin and R. Orbach, *Phys. Rev. B: Condens. Matter*, 1984, **11**, 6514; (*e*) P. H. Lin, T. J. Burchell, R. Clerac and M. Murugesu, *Angew. Chem., Int. Ed.*, 2008, **47**, 8848; (*f*) G. F. Xu, Q. L. Wang, P. Gamez, Y. Ma, R. Clerac, J. Tang, S. P. Yan, P. Cheng and D. Z. Liao, *Chem. Commun.*, 2010, **46**, 1506; (*g*) M. T. Gamer, Y. Lan, P. W. Roesky, A. K. Powell and R. Clerac, *Inorg. Chem.*, 2008, **47**, 6581; (*h*) Q. Zhang, H. Zhang, S. Zeng, D. Sun and C. Zhang, *Chem. Asian J.*, 2013, **8**, 1985; (*i*) S.-Y. Lin, C. Wang, L. Zhao and J. Tang, *Chem. Asian J.*, 2014, **9**, 3558.

25. (*a*) C.-S. Liu, M. Du, E. Carolina Sañudo, J. Echevarría, M. Hu, Q. Zhang, L.-M. Zhou and S.-M. Fang, *Dalton Trans.*, 2011, **40**, 9366; (*b*) E. Colacio, J. Ruiz-Sánchez, F. J. White and E. K. Brechin, *Inorg. Chem.*, 2011, **50**, 7268.

26. S. Gómez-Coca, A. Urtizbetea, E. Cremades, P. J. Alonso, A. Camón and E. Ruiz, F. Luis, *Nat. Commun.*, 2014, **5**, 4300.

27. (*a*) A. Abragam and B. Bleaney, *Electron Paramagnetic Resonance of Transition Ions*; Clarendon Press: Oxford, U.K., 1970; (*b*) R. L. Carlin, *Magnetochemistry*; Springer-Verlag: New York, 1986.

28. K. N. Shirivastava, *Phys. Status Solidi B*, 1983, **117**, 437.

29. E. Colacio, J. Ruiz, E. Ruiz, E. Cremades, J. Krzystek, S. Carretta, J. Cano, T. Guidi, W. Wernsdorfer and E. K. Brechin, *Angew. Chem., Int. Ed.*, 2013, **52**, 9130.

30. (*a*) V. E. Campbell, R. Guillot, E. Rivière, P.-T. Brun, W. Wernsdorfer and T. Mallah, *Inorg. Chem.*, 2013, **52**, 5194; (*b*) L.

Dalton Transactions Accepted Manuscript

Ungur, M. Thewissen, J.-P. Costes, W. Wernsdorfer and L. F. Chibotaru, *Inorg. Chem.*, 2013, **52**, 6328; (*c*) F. Habib, G. Brunet, V. Vieru, I. Korobkov, L. F. Chibotaru and M. Murugesu, *J. Am. Chem. Soc.*, 2013, **135**, 13242; (*d*) J. D. Rinehart and J. R. Long, *Chem. Sci.*, 2011, **2**, 2078; (*e*) L. J. Batchelor, I. Cimatti, R. Guillot, F. Tuna, W. Wernsdorfer, L. Ungur, L. F. Chibotaru, V. E. Campbell and T. Mallah, *Dalton Trans.*, 2014, **43**, 12146.

31. S. Alvarez, P. Alemany, D. Casanova, J. Cirera, M. Llunell and D. Avnir, *Coord. Chem. Rev.*, 2005, **249**, 1693.

32. (*a*) V. E. Campbell, H. Bolvin, E. Rivière, R. Guillot, W. Wernsdorfer and T. Mallah, *Inorg. Chem.*, 2014, **53**, 2598; (*b*) Y.-Z. Zheng, Y. Lan, C. E. Anson and A. K. Powell, *Inorg. Chem.*, 2008, **47**, 10813; (*c*) P.-F. Shi, G. Xiong, B. Zhao, Z.-Y. Zhang and P. Cheng, *Chem. Commun.*, 2013, **49**, 2338.

33. B. Chakraborty, P. Halder, S. Chakraborty, O. Das and S. Paria, *Inorg. Chim. Acta.,* 2012, **387**, 332.

34. G. Gümrükçü, G. K. Karaoğlan, A. Erdoğmuş, A. Gül and U. Avcıata, *Dyes Pigm.,* 2012, **95**, 280.

35. A.-X. Zhu, J.-P. Zhang, Y.-Y. Lin and X.-M. Chen, *Inorg. Chem.,* 2008, **47**, 389.

36. S. Basak, S. Sen, S. Banerjee, S. Mitra, G. Rosair and M. T. G. Rodriguez, *Polyhedron,* 2007, **26**, 5104.

37. B. Valeur, *Molecular Fluorescence. Principles and Aplications* Wiley-VCH: Weinheim, Germany, 2002, 155.

38. W. A. Melhuish, *J. Phys. Chem.,* 1961, **65**, 229.

39. (*a*) G. M. Sheldrick, *SHELXS-97, Program for X-ray Crystal Structure Solution*, University of Göttingen, Germany, 1997; (*b*) L. J. Farrugia, *J. Appl. Crystallogr.*, 1999, **32**, 837.

40. O. Kahn, *Molecular Magnetism*, VCH Publishers Inc., 1991.

41. P. E. Kruger, N. Martin and M. Nieuwenhuyzen, *J. Chem. Soc., Dalton Trans.*, 2001, 1966.

Dalton Transactions Accepted Manuscript

Table of Contents
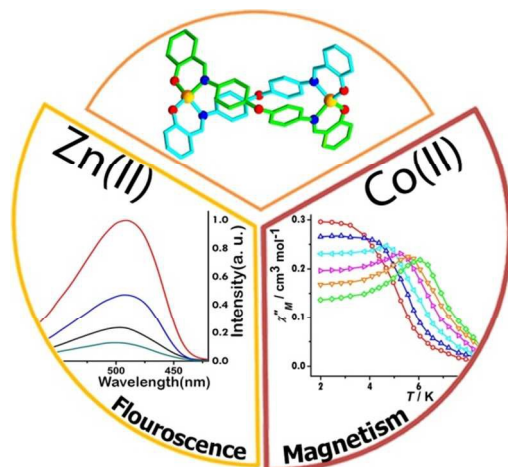
It has been demonstrated that the slow relaxation of magnetization can be achieved in the high spin tetrahedral Co^{II} centres with an easy-plane magnetic anisotropy within the double-stranded helicates. The photoluminescent properties of the Zn analogues were studied in different solvents.